DOI: 10.13009/EUCASS2017-498

The control optimization of low-orbit spacecraft with electric ramjet

Alexander Filatyev, Olga Yanova**
**Central Aerohydrodynamic Institute (TsAGI)*
1 Zhukovsky Str., Zhukovsky, Moscow Reg., Russia

Abstract

The problem of optimal control by the thrust vector of spacecraft (SC) with electric ramjet (ER) to change the orbital parameters is considered. Optimal control is determined by solving the problem on the conditional maximum of the local (at the current point) impact of the perturbing acceleration on the functional, assuming the perturbations' smallness compared to gravity.
An approximate synthesis of the optimal thrust vector is obtained. The investigation results are given depending on the available capacity of the power source, parameters of the SC with ER and initial orbit.

1. Introduction

Electric ramjets (ER) are among upcoming trends in the long-term low-orbit spacecraft (SC). The ER use atmospheric air as the working fluid (WF) and offer a number of feasible advantages, such as long-term operation on the low and extremely low orbits, reduced energy consumption at insertion due to the low orbit and no need for the initial SC propellant margin.
The atmospheric air has long been discussed as a working fluid (see [1], [2]). Nowadays, both Russian and international researchers proceed with studies into the feasibility of electrojet engines ingesting atmospheric air [3], [4]. There are papers dwelling upon optimal control of low-orbit spacecraft with ER. Papers [5], [6] analyzed ER thrust vector optimal control based on the Pontryagin principle maximum aimed to maintain a circular SC orbit and optimal orbit parameters.
This paper presents results obtained from the studies into ER thrust optimal control aimed at the fastest change of the SC orbital parameters (the apogee altitude and inclination) with regard to the limited powerplant (PP) power. The initial stage of this research was presented in the work [7].

2. Electric ramjet scheme

The ER diagram is shown in figure 1. The atmospheric air passes through the air intake (1), accumulates in the WF chamber (2) and then gets to the ion-production chamber (3). The ionized gas speeds up within the accelerator (4) to be neutralized by a flow of electrons (5) and then injected through the nozzle (6) thus generating exhaust thrust. The required power supplies from the PP, either an electric battery, nuclear reactor, or a solar cell battery. Within the present problem statement, it is of crucial importance whether the PP consumes energy or fuel reserved before the launch, or refills energy from practically inexhaustible outsourcing, although under certain limitations.

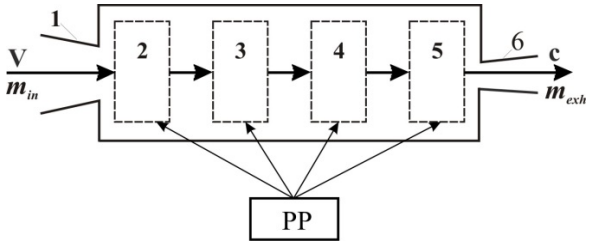

Figure 1: Electric ramjet diagram

DOI: 10.13009/EUCASS2017-498

3. Spacecraft low-orbiting conditions

Let's employ the momentum conservation law in order to estimate the orbit altitude range available for ER-power compensation of the aerodynamic drag [8]:

$$M\Delta V = m_{exh}c - m_{in}V, \tag{1}$$

where M is SC mass, m_{exh} is mass of particles exhausted from the engine nozzle, m_{in} is mass of particles captured in the WF chamber, c is exhaust velocity.

Let $m_{exh} = k_1 m_{in}$, where $0 \le k_1 \le 1$ is the WF mass utilization factor. From (1) then follows the necessary condition for the SC low orbiting ($\Delta V \ge 0$)

$$c \ge V/k_1 . \tag{2}$$

Beside condition (2), the long-term ER-powered SC low orbiting requires admissible thermal fluxes and PP energy. The power generated to accelerate the WF to the velocities sufficient to maintain a circular orbit with regard to condition (2) is determined by

$$W_e \ge \frac{S_{in}\rho V^3}{2\eta k_1}, \tag{3}$$

where η is the ER efficiency factor, ρ is the atmospheric density. The SC sectional area is assumed equal to the intake inlet S_{in} , while the SC solid length is negligible compared with the receptor module.

As it follows from the Kemp-Riddle formula, the minimum apogee altitude h_T where thermal fluxes are within the admissible margin is determined by

$$\bar{\rho}(h_T) \le \bar{q}^2 \bar{V}^{-6}, \tag{4}$$

where $\bar{q}$ is the maximum admissible thermal flux related to q_*, a thermal flux at a certain characteristic circular orbit (CCO) with a radius R_* and an altitude h_*, $\bar{V} = V/V_*$, V_* is the CCO velocity, $\bar{\rho} = \rho(h)/\rho_*$, $\rho_* = \rho(h_*)$.

With regard to the weak dependence of the orbital velocity on the orbit altitude as compared to the exponential relationship of the atmospheric density, it follows from (3) and (4) that the minimum altitude is determined by the PP-generated energy and thermal flux limitations:

$$\bar{\rho}(h_{\min}) \approx \bar{q}^2 \cdot \min\left\{2\eta k_1 \bar{W}_e / \bar{q}^2 , 1\right\},$$

where $\bar{W}_e = W_e / W_*$, $W_* = \rho(h_*) S_{in} V_*^3$.

The dependence of atmospheric density versus altitude represented by

$$h = h_* + a\ln\bar{\rho} + b(\ln\bar{\rho})^2 + c(\ln\bar{\rho})^3 \tag{5}$$

with $a = -4.55421$ km, $b = 0.00283361$ km, $c = -0.141198$ km is a decent approximation of the Standard Atmosphere [9] within the altitude range of 80 ÷ 300 km. Approximation (5) enables construction of the minimum apogee lines $h_{\min}$ on the plane of parameters $\lg\bar{q}$ and $\lg w$ (figure 2), where

$$w = 2\eta k_1 \bar{W}_e \tag{6}$$

Bearing this dependence in mind the minimum-altitude circular orbits are derivable for the long-term operation of the ER-powered SC with an assigned power. Thus with W_e=500 W, $S_{in} = 1\,\text{m}^2$, $\eta = k_1 = 0.9$, $h_T \le 120$ km we obtain lg w=-2.52 and find $h_{\min} = 155k$m from figure 2. Inversely, derivable is the power necessary to maintain the SC assigned orbit parameter, e.g. for $h_{\min} = 120$ km it follows from figure 2 lg w=-1.42 and then determine the required power for the same flight conditions W_e=6.3 kW, which is an order higher than the value of the previous example with the orbit altitude of 155 km.

DOI: 10.13009/EUCASS2017-498

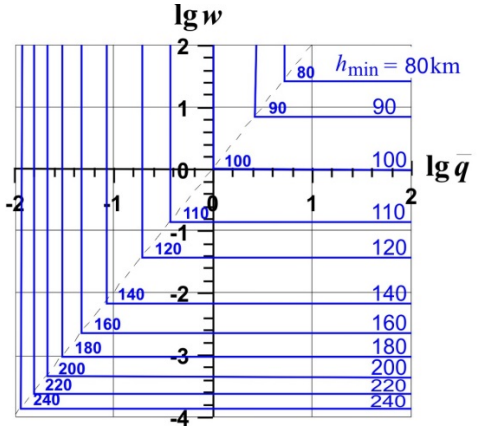

Figure 2: ER-powered SC orbit minimum apogee lines on the plane of parameters $\lg w$ and $\lg \bar{q}$ characteristic of the PP-generated energy and maximum admissible thermal flux

4. Optimization problem statement

The motion of the SC centre of gravity (c.g.) is described in the inertial Cartesian coordinates *Oxyz*c with the origin in the centre of the Earth. The *Oxz* coordinate plane coincides with the plane of the SC initial orbit. The *Oy* axis is directed to the perigee of the initial orbit (in case of a circular orbit it is the SC initial radius vector), the *Ox* axis is directed along the initial velocity vector, the *Oz* axis is aligned with the SC initial angular momentum vector.
Let's write the SC c.g. motion equations in dimensionless form:

$$\begin{cases} \dot{\mathrm{r}} = \mathrm{V}, \\ \dot{\mathrm{V}} = \mathrm{a} - \mathrm{r}/r^3, \\ \dot{m} = \mu, \end{cases}$$

where **r** is the radius-vector related to the CCO radius, **V** is the velocity vector related to the CCO speed, m is WF mass related to the SC initial mass M_i, $\mathbf{a} = \mathbf{P} + \mathbf{A}$ is the disturbing acceleration vector, $\mathbf{P} = P\mathbf{e}_p$ is the thrust-generated acceleration vector, $\mathbf{e}_P$ is the thrust unit vector, $\mathbf{A}$ is the aerodynamic acceleration vector, μ is the WF rate of change related to the characteristic parameter $\mu_* = m_i\sqrt{g_*/R_*}$, g_* is the CCO gravitational acceleration, t is time related to the characteristic time $T_*/2\pi = \sqrt{R_*/g_*}$, T_* is the CCO orbit time, $\dot{()} = d(\,)/dt$.
There are a few assumptions:
1. The SC mass variation is negligible.
2. If the normal air force is negligible, then $\mathbf{A} = -D\mathbf{e}_V$, where $D = 0.5C_x S_{in}\rho V^2$, $\mathbf{e}_V = \mathbf{V}/V$, and

$$\mathbf{a} = P\mathbf{e}_P - D\mathbf{e}_V . \tag{7}$$

3. $W_\mathrm{e} = const$, $c = const$.
The thrust vector **P** is used as a control.
The WF rate of change μ is determined by the difference between the WF rate of arrival to the WF chamber $\mu_{in} = k_1\rho S_{in}V$ and the WF discharge rate through the nozzle μ_{exh}: $\mu = \mu_{in} - \mu_{exh}$. This discharge rate $\mu_{exh} = P/c$ is limited by value of μ_{in} and the PP power W_e (3):

$$0 \le \mu_{exh} \le \mu_{exh\ \max} = \min\left\{\mu_{in},\ 2\eta W_e/c^2\right\}. \tag{8}$$

Based on (8), the thrust limit can be written in the following form:

$$0 \le P \le P_{\max} = \mu_{exh\ \max} c . \tag{9}$$

DOI: 10.13009/EUCASS2017-498

Two optimization problems are under consideration: SC thrust vector **P** control bounded with condition (9) in order to maximize variation of the apogee radius r_α (**Problem I**) or inclination i_{orb} (**Problem II**) within the orbital period *T*.

In view of the negligible disturbing acceleration, let's replace the above-mentioned problems with finding a maximum for the local efficiency of the osculating orbit instant variation, i.e. solution to the thrust vector **P** control with regard to (9) enabling:

Problem I. maximum variation of the apogee radius r_α

$$\Phi_I = \left| \frac{dr_\alpha}{dt} \right|_{r_\pi = const} \Rightarrow \max_{\mathbf{P}}, \tag{10}$$

Problem II. maximum variation of inclination i_{orb}

$$\Phi_{II} = \left| \frac{di_{orb}}{dt} \right|_{\substack{r_\pi = const \\ r_\alpha = const}} \Rightarrow \max_{\mathbf{P}}. \tag{11}$$

Noteworthy, that this simplified problem statement does not involve the motion equations, but representation of the functional only. The approximately optimal solutions we thus obtain are less than strictly optimal ones of the original problem statement in terms of the functional; whereas the approximately optimal solutions have a smaller domain of existence than those in the original statement. Because of this, the below analytical solutions can serve an applicable math tool for the lower-bound estimates of the original problems functional, while analytical synthesis of the approximately optimal control is that, which ensures feasibility of such lower estimates.

5. Maximizing the apogee radius variation

The radii of apogee r_α, perigee r_π, and SC orbit inclination i_{orb} are determined by the following equations [10]:

$$r_\pi = \frac{C^2}{1+e},\ r_\alpha = \frac{C^2}{1-e},\ i_{orb} = \arccos\left(\mathbf{e}_\omega, \mathbf{e}_C\right), \tag{12}$$

where $C = |\mathbf{C}| = |\mathbf{r} \times \mathbf{v}|$, e is the orbit eccentricity, $\mathbf{e}_C = \mathbf{C}/C$, $\mathbf{e}_\omega$ is the unit vector of the angular Earth velocity.

Let us find the thrust vector $\mathbf{P}^+_{opt}$ for the fastest rate of increasing the osculating orbit radius

$$\Phi_I = \left| \frac{dr_\alpha}{dt} \right|_{r_\pi = const} \Rightarrow \max_{\mathbf{P}}. \tag{13}$$

With the $r_\pi = const$ we obtain from (12):

$$\begin{cases} \dfrac{dr_\pi}{dt} = \dfrac{(\mathbf{a}, \mathbf{n})}{e} = 0, \\ \left. \dfrac{dr_\alpha}{dt} \right|_{r_\pi = const} = \left(\dfrac{2r_\pi}{2r_\pi - C^2} \right)^2 (\mathbf{a}, \mathbf{u}) \Rightarrow \max, \end{cases} \tag{14}$$

where $\mathbf{n} = \left(r^2 - r_\pi^2\right)\mathbf{V} - (\mathbf{r}, \mathbf{V})\mathbf{r}$, $\mathbf{u} = \mathbf{C} \times \mathbf{r} = r^2\mathbf{V} - (\mathbf{r}, \mathbf{V})\mathbf{r}$.

Two conditions are analyzed: 1) $P_{\max} > D$, 2) $P_{\max} \le D$.

DOI: 10.13009/EUCASS2017-498

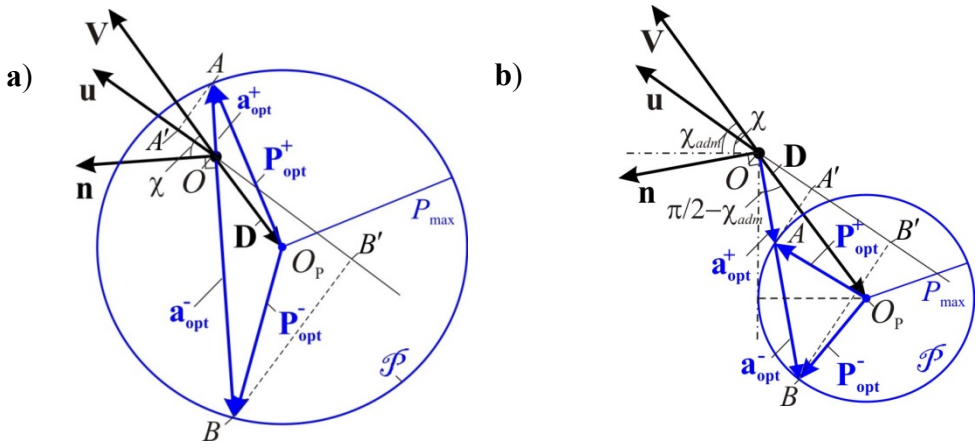

Figure 3: Optimum control for conditions **a**) $P_{\max} > D$ and **b**) $P_{\max} \le D$

Condition 1) is shown in figure 3a. The velocity vector **V** is drawn in-plane from the reference point O in the spacecraft c.g., and the drag vector **D** is drawn contrariwise. The circumference $\mathcal{P}$ of center O_P and radius $P_{\max}$ drawn about the tip of vector **D** is the boundary for the vector **a** tolerance region according to (7) for the current values of **D** and $P_{\max}$. The orthogonality condition (14) reduces the **a** tolerance region down to the secant line AB perpendicular to vector **n**. Points A and B correspond to the maximum OA' and minimum OB' projections of vector **a** on vector **u**. As it follows from (13) and (14), the optimal vectors $\mathbf{P}^+_{opt}$ and $\mathbf{a}^+_{opt}$ arrive at point A.

For the second condition 2) (see figure 3b), solutions obey the same requirements however they do not necessarily exist: the domain of existence for the allowable vectors **a** (7) is shown in figure 3b with a chain-dotted line at an angle $\pi/2 - \chi_{adm}$ with vector **D**. The boundary of the χ_{adm} angle is also shown with a chain-dotted line. The solution exists at

$$\frac{P_{\max}}{D} \ge \cos\chi = \frac{(\mathbf{n},\mathbf{V})}{n\cdot V} = \frac{\bar{r}^2\cos^2\theta - 1}{U}, \tag{15}$$

where θ is angle of projection, χ is angle between vectors **n** and **V**, $U = \sqrt{\left(\bar{r}^2 - 1\right)^2\cos^2\theta + \sin^2\theta}$, $\bar{r} = r/r_\pi$.

The optimal vectors $\mathbf{P}^+_{opt}$ and $\mathbf{a}^+_{opt}$ also correspond to the maximum projection of vector **a** on vector **u**, however here r_α decreases at a minimum rate rather than increases.

Based on (14) and from figure 3 we obtain synthesis of optimal control for **Problem I** (10) for the case (13)

$$\begin{aligned}
&\mathbf{a}^+_{opt} = a^+_{opt}\cdot\mathbf{e}^+_{a\,opt},\ \mathbf{P}^+_{opt} = \mathbf{a}^+_{opt} - \mathbf{D},\\
&a^+_{opt} = \sqrt{P^2_{\max} + D^2\cos^2\chi} - D\sin\chi,\\
&\mathbf{e}^+_{a\,opt} = \frac{\left(\bar{r}^2\cos^2\theta - 1\right)\mathbf{e}_r + \sin\theta\cdot\mathbf{e}_V}{\cos\theta\cdot U}\,sign\theta,
\end{aligned} \tag{16}$$

where $\mathbf{e}_r = \mathbf{r}/r$, $\sin\chi = \bar{r}^2\sin\theta\cdot\cos\theta/U$.

The local efficiency of the apogee radius variation in the dimensionless form is obtained from (14) with regards to (16):

$$\frac{dr_\alpha}{dt} = \frac{4a^+_{opt}C^4V_\pi\sin\theta}{\left(1-e^2\right)^2 U}. \tag{17}$$

Formulae (15)-(17) contain singularities in the orbit perigee which can be removed if expressed by the true anomaly function υ

DOI: 10.13009/EUCASS2017-498

$$\mathbf{e}^{+}_{a\,opt} = \cos\chi \cdot sign(\sin\upsilon)\cdot \mathbf{e}_r + \frac{(1+e\cos\upsilon)}{(1+e)^2}\sin\chi\cdot\mathbf{e}_V,\ \frac{dr_\alpha}{dt} = \frac{4a^{+}_{opt}C^3\sqrt{1+\cos\upsilon}}{(1-e)^2 Z},$$
$$\sin\chi = \frac{(1+e)^2\sqrt{1+\cos\upsilon}}{YZ},\ \cos\chi = \frac{2\sqrt{1-\cos\upsilon}(1+e\cos\upsilon)}{YZ}, \qquad \textbf{(18)}$$

where $Y = \sqrt{1+e^2+2e\cos\upsilon}$, $Z = \sqrt{(1+e)^2(1+\cos\upsilon)+4(1-\cos\upsilon)+2e\left(1-\cos^2\upsilon\right)}$.

As is seen from (17), (18) the ER effectiveness depends on the SC orbital position and varies within the following range:

$$\min_t \frac{dr_\alpha}{dt} = 0,\ \max_t \frac{dr_\alpha}{dt} = \frac{4r_\pi r_\alpha^2\sqrt{P_{\max}^2+D^2}}{C^3},$$

where the extremes are reached in the apogee and perigee accordingly.

The thrust vector $\mathbf{P}^{-}_{opt}$ for the fastest decrease in the apogee radius of an osculating orbit

$$\Phi_I = \left.\frac{dr_\alpha}{dt}\right|_{r_\pi = const} = \left(\frac{2r_\pi}{2r_\pi - C^2}\right)^2(\mathbf{a},\mathbf{u}) \Rightarrow \min_{\mathbf{P}},$$

is obtained similar to functional (13) (see figure 3):

$$\mathbf{a}^{-}_{opt} = a^{-}_{opt}\cdot\mathbf{e}^{-}_{a\,opt},\ \mathbf{P}^{-}_{opt} = \mathbf{a}^{-}_{opt} - \mathbf{D},$$
$$a^{-}_{opt} = \sqrt{P_{\max}^2 + D^2\cos^2\chi} + D\sin\chi,$$
$$\mathbf{e}^{-}_{a\,opt} = -\frac{\left(\bar{r}^2\cos^2\theta - 1\right)\mathbf{e}_r + \sin\theta\cdot\mathbf{e}_V}{\cos\theta\cdot U}\,sign\,\theta.$$

Thus obtained optimal control effectiveness is worth comparing with the extreme event of the apogee radius variation Δr_α^{imp} due to the optimal thrust impulse. The impulse of velocity ΔV is determined by Tsiolkovsky formula, where the mass flow is taken equal to the WF mass hypothetically accumulated over an orbital period T on the original orbit:

$$\Delta V = c\ln\frac{1}{1-\Delta m} \approx c\Delta m, \qquad \textbf{(19)}$$

where $\Delta m = \int_0^T \mu_{exh}dt = k_1 S_{in}\int_0^T \rho(h)Vdt$.

Δr_α^{imp} is determined by formula

$$\Delta r_\alpha^{imp} = -\frac{1}{V_\pi^2 - 2/r_\pi} + \sqrt{\frac{1}{\left(V_\pi^2 - 2/r_\pi\right)^2} + \frac{V_\pi^2 r_\pi^2}{V_\pi^2 - 2/r_\pi}}.$$

The effectiveness of the optimal pulse variation in the apogee radius is accordingly expressed as $\Phi_r^{imp} = \Delta r_\alpha^{imp}/T$.

The optimal pulse moment and direction are to be obtained from the above relations as they are based on the local, or de facto, pulse optimization. In particular, the optimal pulse moment for functional (10) is applied in the orbit perigee, while its optimal direction is tangent to the trajectory (for Φ_I^{+} it is along the velocity vector, and for Φ_I^{-} it is directed contrariwise).

DOI: 10.13009/EUCASS2017-498

6. Maximizing the rate of change of the orbit inclination

Let us write statement of **Problem II** (11) with regard to (12):

$$\left.\frac{di_{orb}}{dt}\right|_{\substack{r_\pi=const\\ r_\alpha=const}} = \frac{(\mathbf{a},\mathbf{r}_\omega)}{C\sqrt{1-(\mathbf{e}_C,\mathbf{e}_\omega)^2}}\, sign(\mathbf{e}_C,\mathbf{r}_\omega) \Rightarrow \max_{\mathbf{P}}. \tag{20}$$

Under condition (11) it follows from (14) that $\mathbf{a}\perp\mathbf{n}$, $\mathbf{a}\perp\mathbf{V}$, which means that

$$\mathbf{a}\,\|\,\mathbf{e}_C, \tag{21}$$

and according to (7), the optimal thrust vector $\mathbf{P}_{opt}$ lies within the plane of vectors $\mathbf{C}$ and $\mathbf{V}$, and can be expressed in the following way

$$\mathbf{P}_{opt} = P_{\max}\left(\cos\varphi\cdot\mathbf{e}_V + \sin\varphi\cdot\mathbf{e}_C\right),$$

Where φ is the angle between vectors $\mathbf{P}_{opt}$ and $\mathbf{V}$, $\cos\varphi = (\mathbf{e}_{P\,opt},\mathbf{e}_V)$, $\sin\varphi = (\mathbf{e}_{P\,opt},\mathbf{e}_C)$.
Considering for (21), $(\mathbf{a}_{opt},\mathbf{e}_C)$ can be expressed as

$$(\mathbf{a}_{opt},\mathbf{e}_C) = a_{opt} = P_{\max}\sin\varphi \tag{22}$$

and setting this equal to the expression obtained from (7)

$$a_{opt} = \sqrt{P_{\max}^2 + D^2 - 2P_{\max}D\cos\varphi}\,, \tag{23}$$

we thus design control for problem (11)

$$\begin{aligned}\mathbf{P}_{opt} &= \sqrt{P_{\max}^2 - D^2}\, sign(\mathbf{e}_C,\mathbf{r}_\omega)\mathbf{e}_C - \mathbf{D},\\ \mathbf{a}_{opt} &= \sqrt{P_{\max}^2 - D^2}\cdot sign(\mathbf{e}_C,\mathbf{r}_\omega)\cdot\mathbf{e}_C.\end{aligned} \tag{24}$$

According to (20) and (24), the maximum efficient rate of inclination increase is reached on the nodal line [2] at $\upsilon = 2\pi-\omega,\ \pi-\omega$ (ω is the perigee argument), and the minimum efficiency is reached at $\upsilon = 3\pi/2-\omega,\ \pi/2-\omega$:

$$\max_\upsilon\left|\frac{di_{orb}}{dt}\right| = \left.\frac{r}{C}\sqrt{P_{\max}^2 - D^2}\right|_{\upsilon=2\pi-\omega},\ \min_\upsilon\left|\frac{di_{orb}}{dt}\right| = 0.$$

A change in inclination Δi_{orb}^{imp} due to the thrust pulse application at the maximum efficiency point (on the nodal line) depends on the velocity impulse (19) in the direction orthogonal to the orbital plane. Taking in mind that $\Delta V << V$, we find $\Delta i_{orb}^{imp} \cong \Delta V/V$ and the corresponding efficiency of the optimal pulse change of inclination as $\Phi_i^{imp} = \Delta i_{orb}^{imp}/T$.

7. Numerical results

Computational investigation has been performed for the electric ramjet, spacecraft and orbit parameters given in Table 1.

DOI: 10.13009/EUCASS2017-498

Table 1: ER, SC and orbit parameters

Parameter	Variation range
ballistic coefficient $\sigma = C_x S_{\text{in}}/m$, m^2/kg	0.0022
c/V_*	1.3
h_π, km	[100, 200]
h_α, km	[100, 240]
i_{orb}, degree	51.6
$\eta = k_1$	1
R_*, km	6371.25
W_e, W	[200, 1200]

Figure 4 presents data on the angle α_{opt} between the optimal thrust vector $\mathbf{P}_{opt}$ and velocity vector as well as the efficiency of the apogee radius rate related to its pulse change Φ_r^{imp} obtained for the same orbits with the apogee altitude of $h_\alpha = 200$ km: $\frac{\overline{dr_\alpha}}{dt} = \frac{dr_\alpha}{dt} \Big/ \Phi_r^{imp}$. Figure 5 shows angle φ_{opt} between the thrust vector $\mathbf{P}_{opt}$ and orbital plane as well as the efficiency of the inclination rate of change related to the inclination pulse change efficiency Φ_i^{imp} for the same orbit: $\frac{\overline{di_{orb}}}{dt} = \frac{di_{orb}}{dt} \Big/ \Phi_i^{imp}$. The thrust optimal manoeuver is obviously independent of the perigee altitude h_π within this range of variation, whereas efficiency of change in these parameters drops over two times with the increase in h_π from 100 to 200 km due to the higher flight altitude. Data shown in figures 4 and 5 are obtained without regard to the PP power limitation.

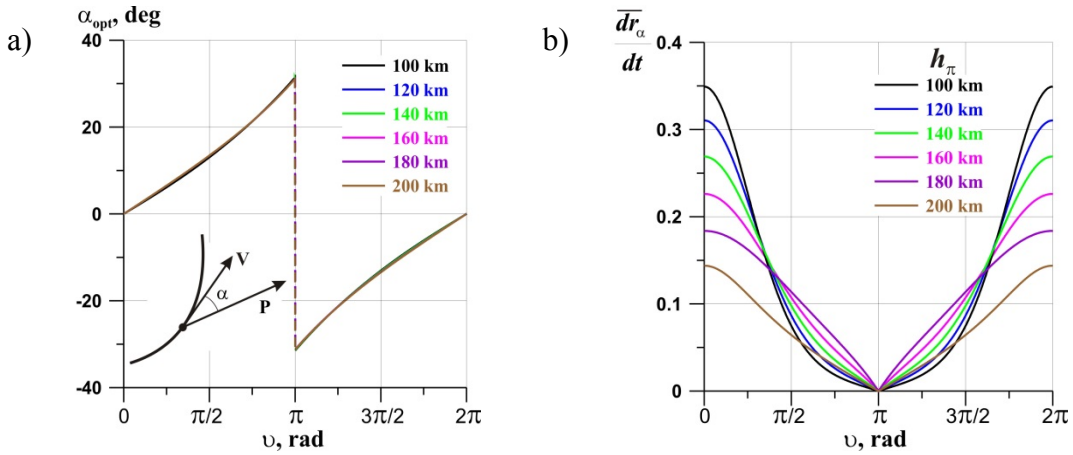

Figure 4: Optimal angle α_{opt} and the efficiency of apogee radius change $\frac{\overline{dr_\alpha}}{dt}$ versus true anomaly υ and perigee altitude h_π in orbits with the apogee altitude $h_\alpha = 200$ km

The efficiency of the apogee radius change over the orbital period versus the dimensionless PP power parameter w (6) is given in figure 6 for orbits with the perigee altitude of $h_\pi \in [100, 200]$ km and apogee altitude of h_α =240 km. The envelope of points of leaving the power restriction indicates the minimum power necessary to accelerate all working fluid incoming the WF chamber for the orbit with an assigned perigee altitude. Increments in the apogee radius are related to its change Δr_α^{100} in the orbit with h_π = 100 km and h_α = 240 km: $\overline{\Delta r_\alpha} = \Delta r_\alpha / \Delta r_\alpha^{100}$.
When the PP power is insufficient to accelerate the entire mass incoming the WF chamber, it is suggested that the accumulated WF at such orbital sections is available for other orbital sections where PP has a power W_e exceeding the required one for the WF acceleration. Figure 7 shows results obtained for the SC flight with the ER thrust optimal control and WF accumulation with the aim to maximize the apogee radius. The SC optimal thrust related to the

DOI: 10.13009/EUCASS2017-498

maximal thrust $\overline{P}_{opt} = P_{opt}/P_{\max}$ (see(9)) is given versus the SC orbital position (true anomaly) with and without regarding the power constraint. Sections marked red are those where the WF is accumulated; this mass is the difference between the WF incoming the WF chamber and that exhausted thru the nozzle in order to generate jet thrust. The green sections are those where the accumulated WF is consumed along with the WF mass currently incoming from the intake. The apogee radius increments are related to its change without WF accumulation. It is obvious that accumulation of the WF mass leads to over two times higher efficiency of the apogee radius change.

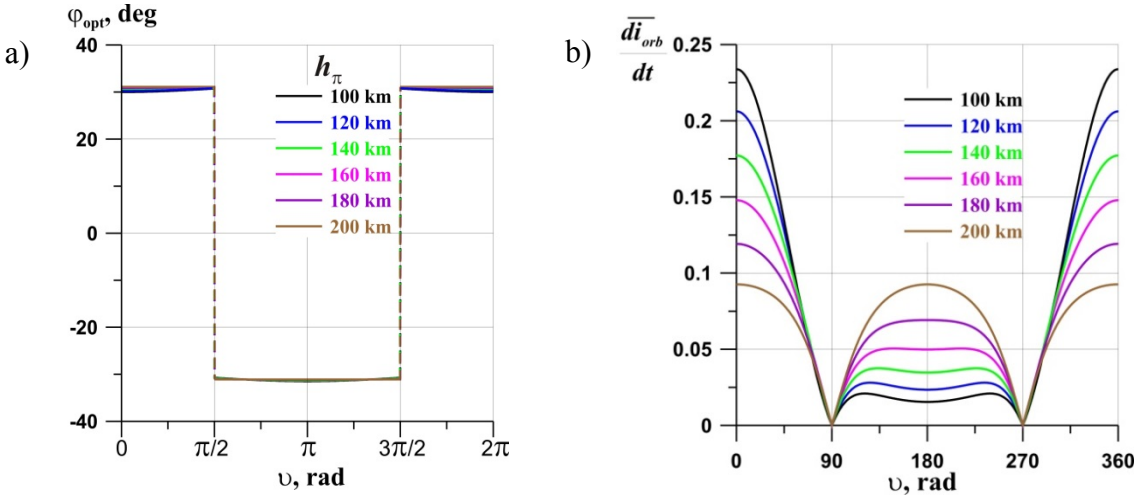

Figure 5: Optimal angle φ_{opt} between the thrust vector $\mathbf{P}_{opt}$ and orbital plane & dimensionless inclination change efficiency $\frac{\overline{di_{orb}}}{dt}$ versus true anomaly υ and perigee altitude h_π in orbits with the apogee altitude h_α = 200 km

Conclusions

Optimization of the ER thrust vector control has been considered with the purpose of changing a spacecraft orbit apogee radius and inclination.

The proposed analytical approach to the electric ramjet control makes it possible to design analytical relations and estimate control efficiency for the orbit apogee and inclination depending on the spacecraft orbital position and powerplant available power.

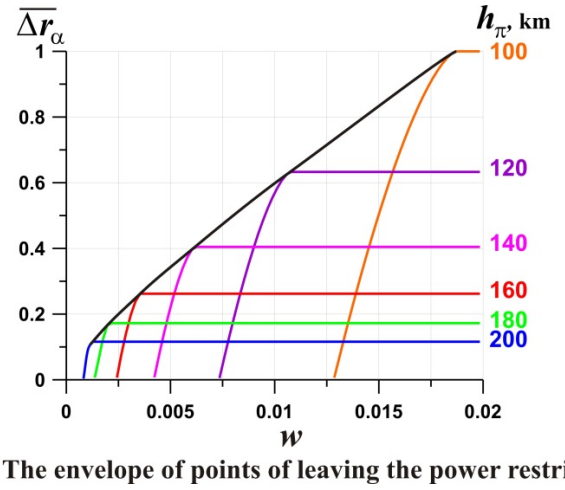

Figure 6: The apogee radius change $\overline{\Delta r}_\alpha$ versus dimensionless parameter w (6), characterizing the PP power W_e, and perigee altitude h_π at h_α = 240 km

DOI: 10.13009/EUCASS2017-498

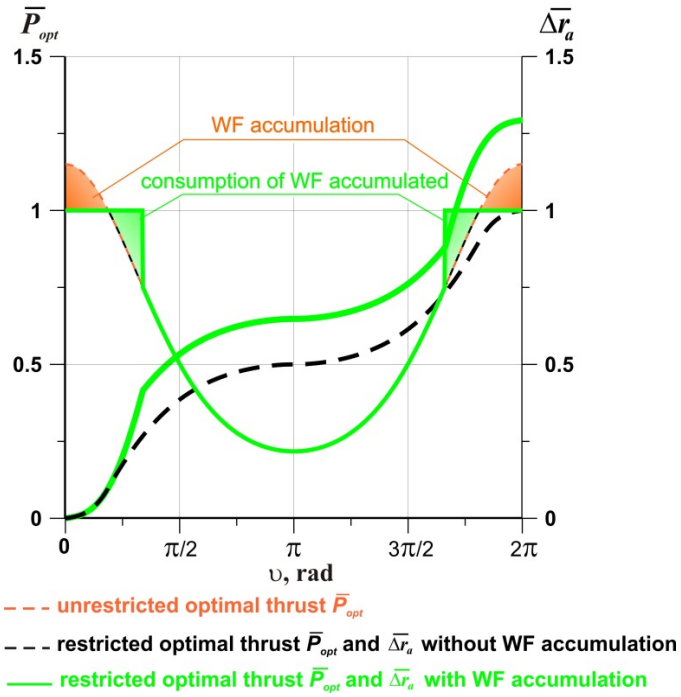

Figure 7: The apogee radius change $\Delta\bar{r}_\alpha$ with the ER thrust optimal control and WF accumulation at the orbit with h_π = 180 km and h_α = 240 km

References

[1] Demetriades S.T. A. novel system for space flight using a propulsive fluid accumulator. 1. British lnterplanetary Society, Vol. 17, № 5, 1959.

[2] Grodzovsky G.L.,Ivanov Y.N., Tokarev V.V. Mechanics of space flight with low thrust. M.: «Nauka». 1966 (in Russian).

[3] DiCara D., Gonzalez del Amo J., Santovincenzo A., et.al. RAM Electric Propulsion for Low Earth Orbit Operation: an ESA study / 30th International Electric Propulsion Conference, Sept. 2007, IEPC-2007-162.

[4] Erofeev A.I., Nikiforov A.P., Popov G.A., Suvorov M.O., Syrin S.A., Khartov S.A. Air-electrorocket ramjet for compensating of low-orbit spacecraft aerodynamic drag. Vestnik NPO imeni S.A. Lavochkina, 2016, № 3. 104-110.

[5] Tsoi E.P. Deciding on optimal control of the work fluid thrust in transient modes. Trudy TsAGI, iss. 1145, 1968.

[6] Shumilkin V.G. Thrust control of an orbiter with a limited-power engine in flight with accumulation of atmospheric air. TsAGI Science Journal. 1976. Vol. XII. Iss. 2: 81-87.

[7] Filatyev A.S., Yanova O.V. On the optimal use of electric ramjet for low-orbit spacecraft. http://www.journals.elsevier.com/procedia-engineering. 2016.

[8] Marov M.Ya., Filatiev A.S. Integrated research of electrojet engines in Earth's ionosphere: To the 50-th anniversary of State Program “Yantar”. Cosmic Research, 2017 (in press).

[9] Standard Atmosphere. GOST 4401-81.

[10] *Okhotsimsky D.E.,Sikharulidze Yu.G.* Fundamentals of Space Flight Mechanics. M.: «Nauka», 1990 (in Russian).